# Using the HTDP Software to Transform Spatial Coordinates Across Time and Between Reference Frames*

**Richard A. Snay**

**ABSTRACT:** The Horizontal Time-Dependent Positioning (HTDP) software program may be used to predict the velocities and displacements associated with horizontal crustal motion, including that related to plate tectonics and earthquakes. The software may also be used to account for this motion in updating positional coordinates and/or survey observations of one date to corresponding ones for another date. Because HTDP supports these activities for coordinates expressed in the North American Datum of 1983 (NAD 83) as well as for coordinates expressed in any official realization of the International Terrestrial Reference Frame (ITRF), this software may be used to transform 3-dimensional positional coordinates from one reference frame to another in a manner that rigorously addresses the relative motion between these frames.

## Introduction

Promptly after the magnitude 8.3 San Francisco earthquake of 1906, the U.S. Coast and Geodetic Survey dispatched survey teams to reposition hundreds of geodetic marks that had been displaced during that event. That survey represents the first significant involvement of the U.S. geodetic community with crustal motion. The community has since measured displacements for over 30 additional earthquakes, including catastrophic events in Alaska, California, Hawaii, Idaho, Montana, and Nevada. In addition to measuring these episodic-type movements, the geodetic community has been engaged in monitoring continuously accumulating deformation occurring in regions prone to earthquakes, volcanic activity, land subsidence, and postglacial uplift. In combination, these deforming regions comprise a significant portion of the United States. Figure 1 identifies those regions that have deformed within the past few centuries as a result of tectonic plate interactions and major earthquakes (magnitude > 7). The vicinity of the Great Lakes, plus much of Canada and Alaska, are moving steadily upward as these regions continue to rebound from the indentations caused several hundred thousand years ago by massive glacial loads. Also, the vicinity of the Chesapeake Bay is subsiding, as are regions in Arizona, California, Louisiana, and Texas.

**Richard Snay** is a geodesist at the National Geodetic Survey, NOAA, 1315 East-West Highway, Room 8112, Silver Spring, MD 20910. Phone: (301) 713-3205 x 155; Fax: (301) 713-4327. E-mail: <rich@ngs.noaa.gov>.

For several decades since 1906, studying crustal motion was essentially a scientific activity related to understanding earthquakes and other deformational processes. In the late 1970s, however, the National Geodetic Survey (NGS), an office of NOAA's National Ocean Service, realized its need to model crustal motion for strictly geodetic purposes. In particular, NGS was then developing a new spatial reference frame whose accuracy had to be compatible with the precise geodetic observations then being performed with electro-optical distance measuring instrumentation. This new reference frame would come to be known as the North American Datum of 1983 (NAD 83).

Accordingly, NGS developed models of horizontal crustal motion for California and parts of Alaska, Hawaii, and Nevada (Snay et al. 1987). The National Geodetic Survey then applied these numerical models to transform over 100 years of existing geodetic observations to a set of corresponding observations, as if the transformed observations had been performed on 31 December 1983. NAD 83 positional coordinates were then computed from these transformed observations. The NAD 83 position of a geodetic mark, thus, corresponds to its location on this date.

To obtain the mark's horizontal position for another date, one needs to apply an appropriate crustal motion model. The National Geodetic Survey has, therefore, incorporated such models into a software program, called HTDP (Horizontal Time-

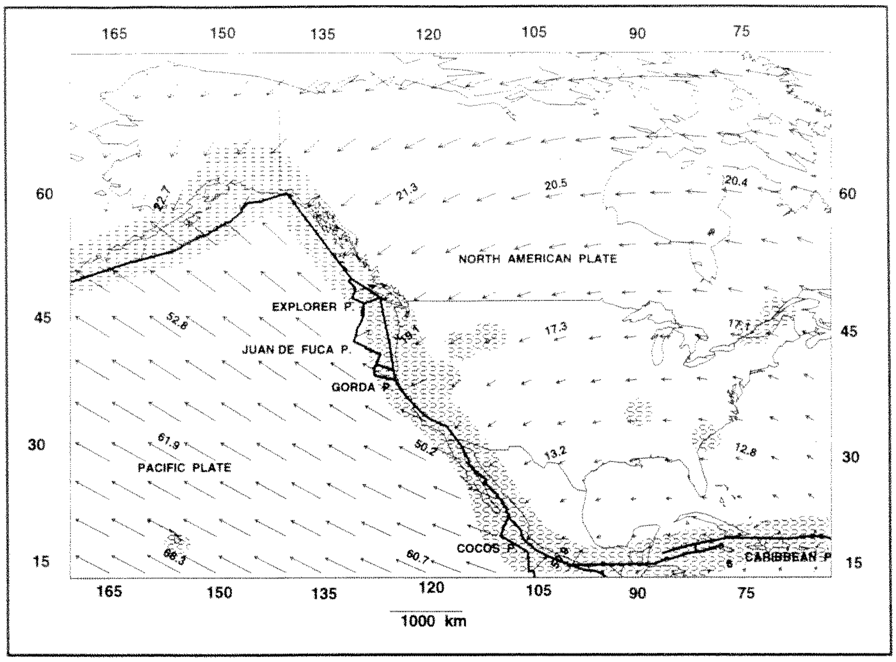


**Figure 1.** Tectonic plates in the vicinity of the United States with predicted ITRF96 horizontal velocities in mm/yr. [Stiple identifies regions that have deformed within the past few centuries as a result of tectonic plate interactions and/or major earthquakes (magnitude >7).]

Dependent Positioning), so that surveyors and others can so update (or backdate) horizontal positions with relative ease. From time to time, NGS upgrades the crustal motion models encoded into HTDP as new measurements are acquired and as the scientific understanding of crustal motion improves.

Updating horizontal positions represents but one application of the HTDP software. The software also enables its users to predict how a point in the United States will move in the future or estimate how it has moved in the past. Also, given a surveying observation measured on one date (a distance, an azimuth, an intermark global positioning system (GPS) vector), HTDP enables its users to predict the corresponding value that would have been measured on a user-specified date. The software handles three-dimensional tasks, such as updating a GPS observation, under the assumption that no vertical motion has occurred. This assumption is required because, for the most part, adequate models for vertical crustal motion are yet to be developed.

Until the 1990s, potential HTDP users practiced their profession in California and a few other deforming regions around the country. The ever growing use of GPS for precise positioning, however, is rapidly expanding the geographic domain of potential HTDP users. Indeed, precise GPS positioning requires that satellite ephemerides be expressed in a reference frame that addresses crustal motion on a global scale. Hence, the International Earth Rotation Service (IERS) has developed the International Terrestrial Reference Frame (ITRF) in which each tectonic plate, including the North American plate, moves continuously (Boucher and Altamimi 1996).

Actually, the IERS has published several realizations of ITRF, namely, ITRF88, ITRF89, ..., ITRF96. Each successive realization incorporates a larger dataset and a more current understanding of error sources to provide more accurate positions and velocities for a worldwide network of geodetic stations. As displayed in Figure 1, horizontal velocities relative to ITRF96 vary in magnitude between 10 and 20 mm/yr in the conterminous 48 states, and horizontal ITRF96 velocities have even greater magnitudes in Alaska and Hawaii. Consequently, the surveying community and others need to consider this motion in relating ITRF positions of one date to those of another date at the accuracy level obtainable with GPS. The National Geodetic Survey enhanced HTDP to support computations in all the official realizations of ITRF as well as in NAD 83, and to enable its users to transform 3-dimensional positional coordinates from one reference frame to another in a manner that rigorously addresses the relative motion between these frames.

## The Nature of Crustal Motion

Although several different physical processes produce crustal motion, HTDP currently addresses only those processes that are tectonic and/or seismic in nature. Also, HTDP addresses only the horizontal components of the associated motion. As the ability to accurately measure deformation improves, the software is likely to encompass additional aspects of crustal motion.

According to the theory of plate tectonics, the Earth's outer shell or crust consists of over 20 plates that overlie a substratum known as the mantle. As radioactivity causes temperatures in the Earth to grow warmer with increasing depth, this temperature gradient induces convective flow within the viscous mantle. The tectonic plates, being relatively stiff, respond to this flow by moving essentially laterally, like rafts floating across the mantle's outer surface.

The above scenario is actually more complicated, especially near interplate boundaries. The physical processes that occur near these boundaries depend on how the adjacent plates move relative to one another. When two plates are moving away from one another, material from the mantle rises and attaches itself to the trailing edges of the diverging plates. As this mantle material cools, its physical characteristics eventually become those of a tectonic plate. Thus, diverging plates are constantly growing in size in the vicinity of their common boundary. Although plate divergence occurs mostly in oceanic regions, it is also occurring in Iceland.

When two plates are moving towards each other, the plate of greater density wedges under the less dense plate. Often, the underthrust plate will subduct or dive deep into the mantle; whereupon it will eventually heat up and assume the physical characteristics of mantle material. Thus, a subducting plate is decreasing in size along its leading edge. Near the United States subduction is occurring along the Aleutian trench, which is located about 250 km south of Alaska's southern coast. Moreover, the Aleutian trench roughly parallels this coastline. Subduction also is occurring along a trench located less than 100 km west of the Pacific coast in Washington, Oregon, and northern California (Figure 1).

The Aleutian trench represents a segment of the boundary between the Pacific plate and the North American plate. Along this trench, the Pacific plate subducts beneath the less dense North American plate, but not without considerable interplate friction. This friction causes both plates to deform across a zone that extends several hundred kilometers outward from the trench. The crumpling plates behave somewhat like two giant springs being compressed. When these plates have been deformed to the point that they store sufficient elastic energy to overcome their interplate friction, both plates will suddenly lunge forward along their respective tectonic paths, giving rise to an associated earthquake. Thus, the tectonic process induces a seismic process.

Plate convergence also occurs near the Pacific coast in Washington, Oregon, and northern California. Here, three small plates—the Gorda plate, the Juan de Fuca plate, and the Explorer plate—subduct along the offshore trench that constitutes their collective boundary with the North American plate. The interior of the Juan de Fuca plate moves at a rate of 42 mm/yr in the N69°E direction relative to the

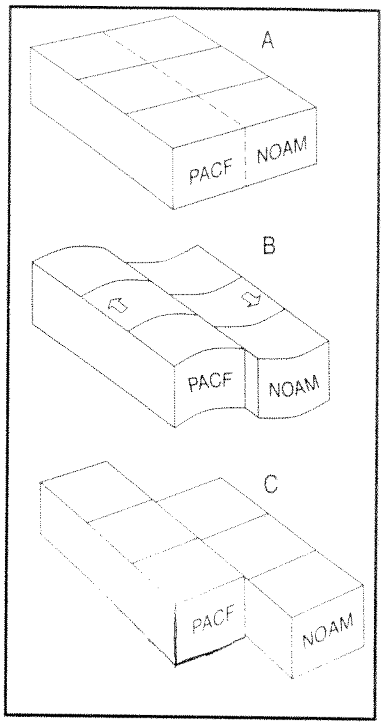


**Figure 2.** The tectonic process in California. (A) Immediately after an earthquake, lines are painted across adjacent plates. (B) At some later time, these lines reveal that the plates have deformed. (C) Immediately after the subsequent earthquake, the lines reveal that the plates have shifted, yet, they have returned to their original shape.

interior of the North American plate (DeMets et al. 1990; 1994). The Gorda plate and the Explorer plate are too small to have had their velocities determined. Onshore deformation manifests itself as contraction in the general direction of relative plate motion at rates on the order of 100 nanostrain per year (nstr/yr); that is, 100 parts in $10^9$ per year (Snay and Matsikari 1991; Savage et al. 1991). Sooner or later, the elastic energy accumulating as a result of this compression will induce a major earthquake. Present day velocities along the coast are approximately 10 mm/yr relative to the interior of the North American plate (Fluck et al. 1997).

In southern California, the relative motion between adjacent plates is oriented nearly parallel to their common boundary. Were there no friction along this segment of the interplate boundary, then the Pacific plate would move northwestward relative to the North American plate at an average rate of about 48 mm/yr along this segment of their common boundary. This relative motion, however, is impeded by friction that may be attributed to the roughness of the plate boundary and/or to local deviation in the boundary's orientation.

Figure 2 presents an idealized depiction of the horizontal motion occurring in southern California. At time $T$ (Figure 2A), several straight lines are painted on the Earth's surface so that they are orthogonal to the interplate boundary, which is represented as a geologic fault having a planar surface. At time $T$ + 10 years (Figure 2B), these lines have deformed into broken curves. Now points on the Pacific plate which are located sufficiently far from the

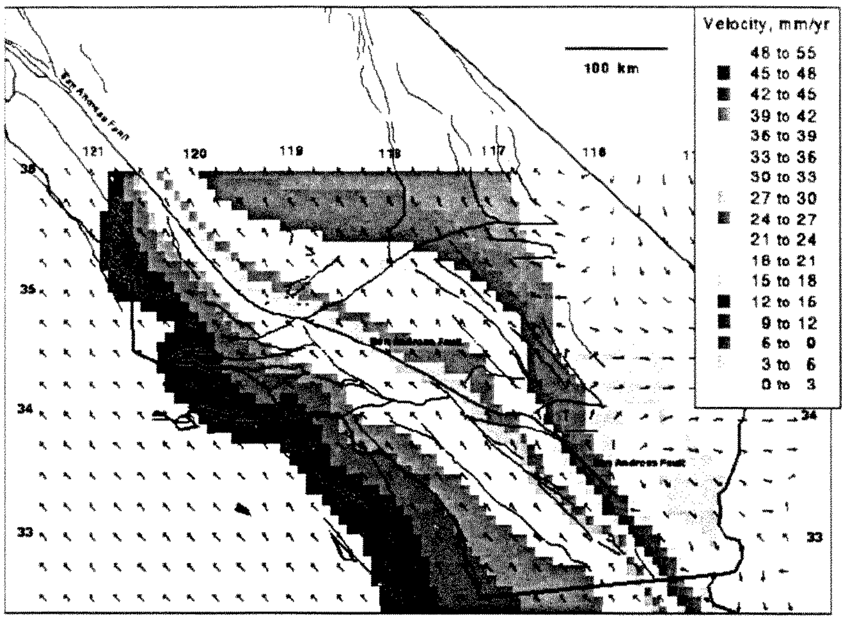


**Figure 3.** Horizontal velocities across southern California based on the results of Shen et al. (1997). [Greyscale shadings specify speeds and arrows specify corresponding directions of motion relative to a fixed North American plate reference frame. Curved lines represent geologic faults according to Jennings (1975).]

interplate boundary have translated 480 mm relative to points on the North American plate, which are also located sufficiently far from the interplate boundary. The slip (i.e., the relative displacement of formerly adjacent points on opposite sides of the fault) equals some amount less than 480 mm. The curvature of the painted lines at time $T + 10$ years reflects the bending that each plate has undergone as a result of interplate friction. At some point in the future, the elastic energy accumulating in these bending plates will become sufficient to overcome this friction. Then, each plate will return to near its undeformed shape with a southern jolt—an earthquake (Figure 2C).

In real life, the situation is considerably more complex, as is revealed by a current estimate of the horizontal velocity field across ~~sudden~~ southern California (Figure 3). This complexity occurs because the interplate boundary is not a single planar geologic fault as depicted in Figure 2, but a collection of geologic faults. Moreover, the surface of each individual fault may possess significant curvature. Some subset of these faults never intersects the Earth's surface. Those faults that do intersect the surface may trace rather sinuous paths across the landscape. Also, individual fault surfaces may be oriented rather obliquely to the overall direction of plate motion. Even the trace of the San Andreas fault, the primary constituent of the interplate boundary in southern California, varies in orientation by about 30° along its extent (Figure 3). Such variations in fault orientation cause noticeable bends in several of the contours of constant speed which are present in Figure 3. Also, these contours do not remain parallel to each other, as would be the case with the idealized motion depicted in Figure 2. The convergence and divergence of these contours is associated both with variations in fault orientation and with spatial variations in the slip rates on the faults. Indeed, even on an individual fault, the ongoing slip rate can exhibit significant spatial variation.

Figure 3 clearly illustrates that the deformation associated with interplate friction can be distributed across an area that extends several hundred kilometers outward from the interplate boundary. At some distance, however, this deformation becomes insignificant. Thus, plate interiors remain relatively undeformed, except where some other physical process (volcanic/magmatic activity, land subsidence, postglacial uplift) is active. Space-based geodetic techniques (GPS, very long baseline interferometry (VLBI), and satellite laser ranging) have indicated that plate interiors remain internally stable at the 3-mm/yr level or better (Argus and Heflin 1995; Dixon and Mao 1996; Larson et al. 1997; Ma and Ryan 1995). Moreover, results from the spaced-based techniques, when combined with geologic results, imply that relative horizontal velocities among different plate interiors have remained remarkably constant over the past 3 million years (DeMets et al. 1994).

## Crustal Motion Models in HTDP

The HTDP software incorporates models that address both the continuous and the episodic components of crustal motion. To characterize continuous motion, the models embody the assumption that points on the Earth's surface move with constant horizontal velocities. This assumption is generally acceptable, except for the accelerated motion

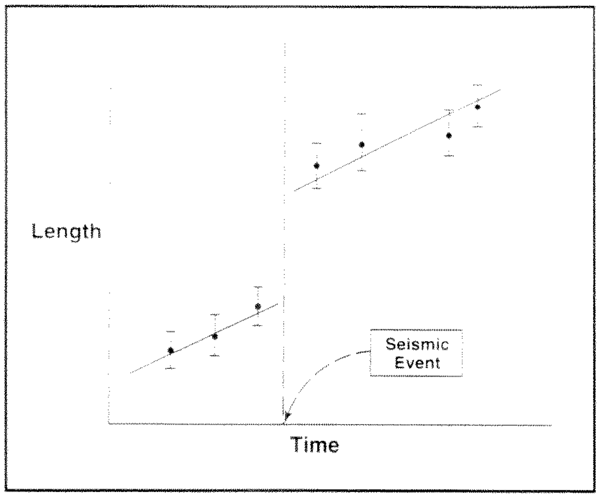


**Figure 4.** Crustal motion models in HTDP assume that the length of a baseline varies linearly with time, except for the instantaneous jumps that occur during earthquakes.

experienced during the years following a major earthquake and for the motion associated with volcanic/magmatic activity.

For characterizing the episodic motion associated with earthquakes, the models embody the assumption that displacements occur instantaneously. Figure 4 illustrates how the length of a baseline might vary over time according to the HTDP models. Internally, the HTDP software expresses all motion relative to the NAD 83 reference frame; wherein the interior of the North American plate does not move on average. The software can, however, convert the motion from this reference frame to several other spatial reference frames.

For the computation of horizontal velocities, several regions of the Earth have been defined, each bounded by a closed polygon. For each region, HTDP stores the horizontal velocities for the nodes of a regularly spaced, 2-dimensional grid[1] as defined by curves of constant latitude and longitude. The program then interpolates among these stored velocities to obtain velocities at other points in the region. Should two regions overlap, then HTDP assigns the points in their intersection to that region whose boundary appears first in its storage scheme. The program displays an error message when it is asked to compute the velocity at a point located outside all of its designated regions.

For the computation of the episodic motion associated with earthquakes, HTDP represents the Earth as an isotropic, homogeneous, elastic body. Rectangular planes of finite dimensions are embedded in this body to represent patches on specific geologic faults. The motion associated with an earthquake corresponds to the deformation that the elastic body undergoes in response to a slip along these rectangular surfaces. This motion is given by the equations of dislocation theory (Okada 1985).

The displacements are a function of the location, size, and orientation of the rectangles, as well as the magnitude and direction of the slip (Figure 5).[2] Figure 6 shows the horizontal displacements predicted by a dislocation model for the magnitude 7.1 Loma Prieta earthquake that occurred just south of San Francisco in 1989. Table 1 identifies the dislocation models encoded into version 2.2 of HTDP. Figure 7 locates the corresponding earthquakes that occurred in California.

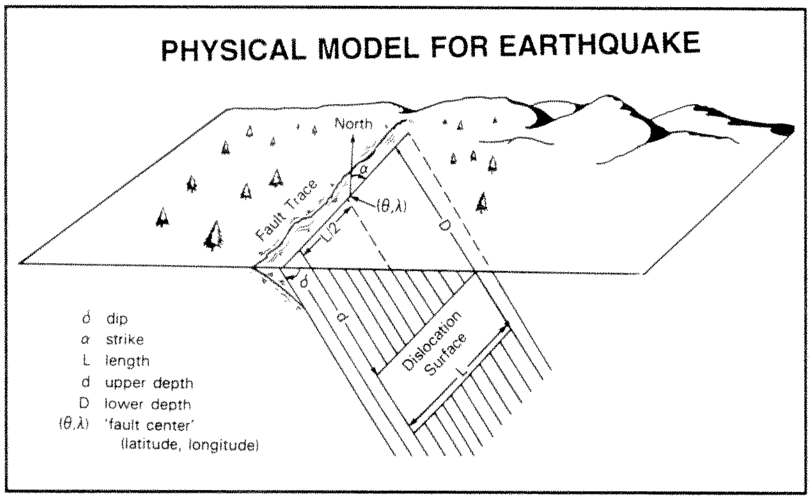


**Figure 5.** Dislocation theory describes how each point in an isotropic, homogeneous, elastic body moves in response to relative slip between opposing faces of a rectangle embedded in this body.

The National Geodetic Survey has upgraded the crustal motion models encoded into HTDP with the help of individuals from many institutions. The software's original version, released in June 1992, incorporated Snay and Herbrechtsmeier' (1994) model which characterizes horizontal velocities across

[1] Grid spacing varies from region to region.

[2] In the HTDP software, it is assumed that the upper and lower edges of the embedded rectangle are parallel to the Earth's surface and the slip vector is constant over the rectangle. Figure 5 identifies a set of parameters sufficient to specify the size, location, and orientation of the rectangle. The motion depends on these parameters, the Poisson ratio of the crust (here assumed to equal 0.25), and the slip vector. The spatial variation of the fault slip is introduced by approximating the fault with several rectangles, each having a constant slip vector.

California plus the episodic displacements associated with 13 California earthquakes. The NGS has since developed 12 subsequent versions of HTDP which, collectively, have introduced dislocation models for 12 additional earthquakes, 11 in California and 1 in Alaska. The subsequent versions have also introduced improved dislocation models for four California earthquakes and an improved velocity model for southwestern California (south of latitude 36°N, west of longitude 117.5°W).

The National Geodetic Survey developed this improved velocity model by adding a significant number of accurate GPS observations to the data that Snay and Herbrechtsmeier (1994) had used and by applying the new estimation technique described by Snay et al. (1996). Also, version 2.2 incorporates the velocity model that Fluck et al. (1997) developed for western Washington, western Oregon, and northwestern California (north of latitude 40°N and west of longitude 121°W). Version 2.3 of HTDP will incorporates the new velocities estimated by Shen et al. (1997) for ~300 sites in southern California (south of latitude 36°N).

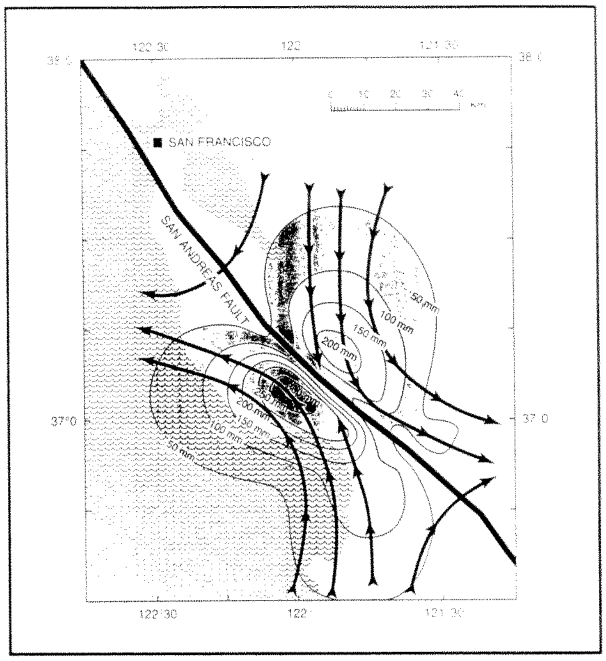


**Figure 6.** Horizontal displacement for the 1989 Loma Prieta earthquake (magnitude 7.1) as derived from pre- and post-earthquake surveys. [Contours indicate the magnitudes of the displacements; flow lines denote the directions of the displacements.]

## Predicting Velocities

When executing the HTDP, the user encounters the following menu:

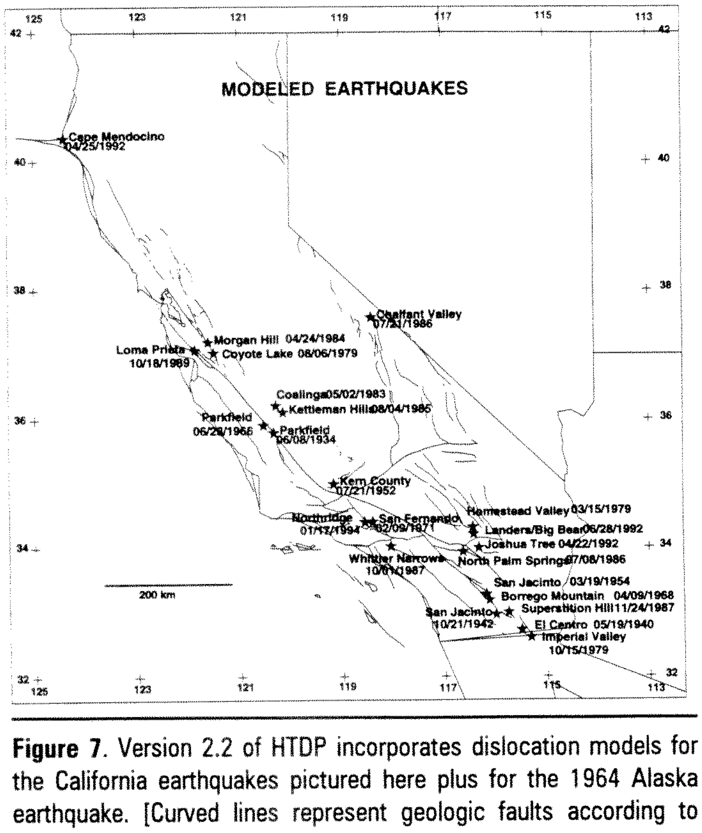


**Figure 7.** Version 2.2 of HTDP incorporates dislocation models for the California earthquakes pictured here plus for the 1964 Alaska earthquake. [Curved lines represent geologic faults according to Jennings (1975).]

0 ... Exit software
1 ... Predict displacements between two dates
2 ... Predict velocities
3 ... Update positions and/or observations to a specified date
4 ... Transform positions between reference frames

Predicting velocities (menu option 2) constitutes the most fundamental HTDP application. To predict a velocity at a point, the user selects a spatial reference frame (NAD 83 or one of the ITRF realizations), specifying the point's positional coordinates in that reference frame. These coordinates can be specified either in terms of geodetic latitude and longitude or in terms of Earth-centered rectilinear X, Y, and Z, where the Z-axis is the Earth's rotational axis (positive north), the positive X-axis points towards longitude 0°, and the positive Y-axis points toward longitude 90°E.

The user can also apply the software to predict velocities for all geodetic points whose coordinates are specified in a given computer file, provided that this file is in "Blue-Book" format (Federal Geodetic Control Subcommittee 1994). Additionally, the user can apply HTDP to predict velocities for the nodes of a user-specified 1-dimensional or 2-dimensional grid located on the Earth's surface. The 1-dimensional case is useful for visualizing how velocity varies along a line segment in a user-specified azimuth. The line segment may or may not correspond to a tangible feature, such as a straight road. The 2-dimensional case is useful for visualizing how velocity varies over a rectangular area on the Earth's surface. Figure 3, for example, was created by contouring the speeds associated with a 2-dimensional grid of velocities in southern California.

National Geodetic Survey staff routinely use HTDP to predict ITRF velocities for new GPS sites (predicted vertical velocities are zero) as these sites are added to the national network of continuously operating reference stations (CORS). With these predicted velocities, NGS is able to provide accurate, up-to-date positions for the CORS on a continuous basis to support those applications requiring cm-level precision. The accuracy of a predicted velocity can be matched by a measured velocity only after two or more years of dedicated monitoring.

In the realm of crustal motion, it is inappropriate to specify positional coordinates for a point without specifying the "epoch date" for the coordinates; i.e., the date to which these coordinates correspond. When HTDP users enter positional coordinates without specifying their epoch date, as is done in predicting velocities, then the software assigns a default epoch date to the specified coordinates.

Currently, the default epoch date is 7 May 1991, which approximates the midpoint of the time interval during which federal, state, and local institutions jointly conducted a high accuracy GPS survey involving ~250 sites distributed throughout California. The HTDP can be used to predict accurate velocities without specifying the epoch date associated with the positional coordinates, because velocity varies rather slowly as a function of position except at points located within a few meters of a major geologic fault, such as California's San Andreas fault.

## Predicting Displacements

Predicting a point's displacements from time $T_1$ to time $T_2$ (menu option 1) involves multiplying the predicted velocity at this point by the time difference ($T_2$ minus $T_1$) and then adding any "instantaneous" displacements that the point experienced as a result of the earthquakes that occurred between these dates. After specifying the two dates—each in terms of year, month, and day—the user selects a spatial reference frame and specifies the point's positional coordinates in that reference frame. As with velocity prediction, these coordinates may be specified interactively, or via a Blue-Book file, or by supplying the attributes of a 1- or 2-dimensional grid on the Earth's surface. Also, as with velocity prediction, the user need not supply the epoch date for the specified positional coordinates. The HTDP assigns its default epoch date, call it $T_0$, to these coordinates. The predicted displacement vector then equals $V_2$ minus $V_1$, where $V_1$ denotes the displacement vector from $T_0$ to $T_1$ and $V_2$ denotes the displacement vector from $T_0$ to $T_2$.

Users should be aware that accuracies of predicted displacements vary greatly in areas where earthquakes have occurred. In many cases, a dislocation model was derived from measured displacements for only a few tens of geodetic sites, whereas the pattern of actual earthquake-related displacements might have been too complex to be characterized adequately by such a small number of measured displacements.

## Updating Positions

When updating a position (menu option 3), the user must specify:

- The reference frame;
- The starting positional coordinates and their epoch date $T_1$ in this reference frame; and
- The date $T_2$ to which the updated coordinates are to correspond.

The HTDP computes the displacement vector from $T_1$ to $T_2$, and adds this vector to the starting positional coordinates to obtain the positional coordinates at time $T_2$. The starting positional coordinates may be entered interactively or via a Blue-Book file. In the latter case, HTDP will create a new Blue-Book file with the updated positional coordinates having replaced the input positional coordinates.

The ability to update positions comes in handy when dealing with a set of surveying observations performed on one date, which involves several control points whose adopted positional coordinates correspond to some other epoch date. In this case, HTDP may be employed to update the positional coordinates of the control points to the survey date, so that these updated coordinates may be used to evaluate the accuracy of the given observations.

In California, the situation is often more complex as positional coordinates for different marks have different epoch dates. For instance, the positional coordinates adopted for most marks in the California High Accuracy Reference Network (HARN), also known as the California High Precision Geodetic Network (HPGN), have an epoch date of 1991.35 (7 May 1991). However, several other

California HARN marks have positional coordinates with more recent epoch dates, reflecting displacement during recent earthquakes (see Table 1 and Figure 7). The HTDP can be applied to update the positional coordinates of all marks to some common date which the user selects.

## Updating Observations

When updating an observation (also menu option 3), such as the measured distance between two sites, the user must specify:

- The type of observation;
- The observed value;
- The date on which the observation was measured;
- The positional coordinates of the associated sites; and
- The date to which the updated observational value is to correspond.

The user enters the last item interactively. The remaining information must be supplied via a Blue-Book file. The program will then create a new Blue-Book file in which the observational records from the input Blue-Book file have been replaced with corresponding records that contain updated values for the observed quantities.

The HTDP program will update various types of observational records contained in a Blue-Book file, including those for distances, azimuths, horizontal directions, horizontal angles, and intermark GPS vectors. Note, however, that the software will not modify the vertical component of an observed intermark GPS vector, because HTDP incorporates the assumption that no vertical motion has occurred. For this same reason, HTDP will not modify observational records for vertical angles and height differences.

The HTDP program computes the updated value of an observed quantity indirectly. Let $D(T_1)$ represent an observed distance between points $A$ and $B$ at time $T_1$. To predict the corresponding distance $D(T_2)$ that would have been measured at time $T_2$, the software will first retrieve positional coordinates for $A$ and $B$ from the positional records (*80* records) in the Blue-Book file. Associating these coordinates with its default epoch date $T_0$, HTDP will update them to corresponding coordinates for $A$ and $B$ at time $T_1$ and then use these updated coordinates to compute the theoretical distance $D^{\#}(T_1)$ between $A$ and $B$ at time $T_1$. Similarly, HTDP will update the starting coordinates for $A$ and $B$ to corresponding coordinates at time $T_2$ to compute the theoretical distance $D^{\#}(T_2)$ at time $T_2$.

The theoretical distance $D^{\#}(T_1)$ can differ from the observed distance $D(T_1)$ for several reasons. First,

| Date | Earthquake (magnitude) | Source of Model |
|---|---|---|
| 07JUN 1934 | Parkfield (M=6.0) | Segall and Du (1993) |
| 17 MAY 1940 | El Centro (M=6.9) | Snay and Herbrechtsmeier (1994) |
| 21 OCT 1942 | San Jacinto (M=6.6) | Snay and Herbrechtsmeier (1994) |
| 21 JUL 1952 | Kern County (M=7.5) | Snay and Herbrechtsmeier (1994) |
| 19 MAR 1954 | San Jacinto (M=6.4) | Snay and Herbrechtsmeier (1994) |
| 26 JUN 1966 | Parkfield (M=5.6) | Segall and Du (1993) |
| 09 APR 1968 | Borrego Mtn. (M=6.5) | Snay and Herbrechtsmeier (1994) |
| 09 FEB 1971 | San Fernando (M=6.6) | Snay and Herbrechtsmeier (1994) |
| 15 MAR 1979 | Homestead Valley (M=5.6) | Stein and Lisowski (1983) |
| 06 AUG 1979 | Coyote Lake (M=5.9) | Snay and Herbrechtsmeier (1994) |
| 15 OCT 1979 | Imperial Valley (M=6.4) | Snay and Herbrechtsmeier (1994) |
| 02 MAY 1983 | Coalinga (M=6.4) | Stein and Ekstrom (1992) |
| 24 APR 1984 | Morgan Hill (M=6.2) | Snay and Herbrechtsmeier (1994) |
| 04 AUG 1985 | Kettleman Hill (M=6.1) | Ekstrom et al (1992) |
| 08 JUL 1986 | N. Palm Springs (M=5.6) | Savage et al. (1993) |
| 21 JUL 1986 | Chalfant Valley (M=6.2) | Savage and Gross (1995) |
| 01 OCT 1987 | Whittier Narrow (M=5.9) | Lin and Stein (1989) |
| 24 NOV 1987 | Superstition Hill (M=6.6, 6.2) | Larsen et al. (1992) |
| 17 OCT 1989 | Loma Prieta (M=7.1) | Lisowski et al. (1990) |
| 22 APR 1992 | Joshua Tree (M=6.1) | Bennett et al. (1995) |
| 25 APR 1992 | Cape Mendocino (M=7.1) | Oppenheimer et al. (1993) |
| 29 JUN 1992 | Landers/Big Bear (M=7.5, 6.6) | Hudnut et al. (1994) |
| 17 JAN 1994 | Northridge (M=6.7) | Hudnut et al. (1996) |
| | ALASKA | |
| 28 MAR 1964 | Prince William Sound (M=9.2) | Holdahl and Sauber (1994) |

**Table 1.** Dislocation models incorporated in the Horizontal Time-Dependent Positioning (HTDP) software.

$D(T_1)$ contains some amount of observational error that is not considered in computing $D^{\#}(T_1)$. Second, the positional coordinates for $A$ and $B$ given in the Blue-Book file might differ from the actual coordinates for $A$ and $B$ at the default time $T_0$. And third, any inaccuracy in the encoded crustal motion models will bias the value of $D^{\#}(T_1)$. For these same reasons, $D^{\#}(T_2)$ will differ from $D(T_2)$, but the difference $D(T_2)$ - $D^{\#}(T_2)$ should approximate the difference $D(T_1)$ - $D^{\#}(T_1)$ in value as both differences involve essentially the same errors. Similarly, the expression $D(T_1) + D^{\#}(T_2) - D^{\#}(T_1)$ should approximate $D(T_2)$. Hence, HTDP sets $D(T_2)$ to the value of this expression. The software updates other types of observations in a similar manner.

The ability to update observations contributes significantly to the software's usefulness. Consider as before a set of surveying observations performed on one date, which involves several control points whose adopted positional coordinates correspond to some other epoch date. Now, instead of updating the positional coordinates of the control points to the survey date, a surveyor can update the observations to the epoch date of the control points. Using these updated observations, the surveyor can easily compute positional coordinates for the other survey points, such that these coordinates have the same epoch date as the coordinates of the control points.

In this same manner, a surveyor can update a collection of surveying observations to a common date even if these observations were performed on various dates that span several decades. Indeed, NGS recently updated over 100 years of existing geodetic observations performed in California to 7 May 1991. Using these updated observations, NGS computed horizontal coordinates for over 10,000 marks, such that these coordinates would be consistent with the coordinates that had been accurately measured in the spring of 1991 for the ~250 marks comprising the California HARN.

## Transforming Positions

In the absence of crustal motion, the equations for transforming positional coordinates from one spatial reference frame to another is rather familiar to the surveying community. Namely, given Cartesian coordinates $(X_1, Y_1, Z_1)$ for a point in the first frame, the corresponding coordinates $(X_2, Y_2, Z_2)$ in the second frame may be computed via the equations:

$$X_2 = T_X + (1+S) * X_1 + R_Z * Y_1 - R_Y * Z_1 \quad (1)$$

$$Y_2 = T_Y - R_Z * X_1 + (1+S) * Y_1 + R_X * Z_1 \quad (2)$$

$$Z_2 = T_Z + R_Y * X_1 - R_X * Y_1 + (1+S) * Z_1 \quad (3)$$

where $T_X$, $T_Y$, and $T_Z$ represent three translations along the X-axis, Y-axis, and Z-axis, respectively, which will bring the origins of the two frames into coincidence. $R_X$, $R_Y$, and $R_Z$ represent three rotation about the X-axis, Y-axis, and Z-axis, which, in combination, will bring the three axes of one frame into parallel alignment with their corresponding axes in the other frame. Finally, S represents the difference in scale between the two frames.

In the presence of crustal motion, the transformation equations can be generalized to allow one frame to move relative to the other. Thus, each of the seven defining parameters becomes a function of time $t$; i.e., $T_X(t)$, $T_Y(t)$, $T_Z(t)$, $R_X(t)$, $R_Y(t)$, $R_Z(t)$, and $S(t)$. One of the simpler generalizations is to assume that each of these seven functions is linear with respect to time. Thus, for example, the X-rotation at time $t$ can be expressed by the equation:

$$R_X(t) = R_x(t_0) + (dR_x/dt) * (t - t_0) \quad (4)$$

where:

$t_0$ = a specified reference time;
$R_X(t_0)$ = the X-rotation at time $t_0$; and
$dR_X/dt$ = the temporal rate at which the X-rotation is changing.

This generalized transformation involves 15 parameters—two parameters for each of the seven linear functions plus the reference time $t_0$. It is this generalization that HTDP incorporates to transform positions among different reference frames (menu option 4).

For illustrative purposes, consider a transformation between NAD 83 positional coordinates and ITRF96 positional coordinates. A point's NAD 83 velocity is expressed as if the North American plate does not move on average. Its ITRF96 velocity, on the other hand, is expressed as if the major tectonic plates move according to the "no-net-rotation" NUVEL-1A model of DeMets et al. (1994). According to this model, the North American plate is rotating counterclockwise at a constant rate about an axis that passes through both the Earth's center of mass and a point on the Earth's surface located slightly west of Ecuador (see Figure 1). The ITRF96 frame is, thus, rotating relative to the NAD 83 frame and *vice versa*. This relative motion may be quantified by specifying appropriate values for the three rotation rates $dR_X/dt$, $dR_Y/dt$, and $dR_Z/dt$. The remaining four rates are not required to quantify this motion.

When transforming from ITRF96 to NAD 83, version 2.2. of the HTDP software uses the equations:

$$T_X(t) = 0.9910\,m \quad (5)$$

$$T_Y(t) = -1.9072\,m \quad (6)$$

$$T_Z(t) = -0.5129\,m \quad (7)$$

$$R_X(t) = [125033 + 258(t - 1997.0)]\,(10^{-12})\,radians \quad (8)$$

$$R_Y(t) = [46785 - 3599(t - 1997.0)]\,(10^{-12})\,radians \quad (9)$$

$$R_Z(t) = [56529 - 153(t - 1997.0)]\,(10^{-12})\,radians \quad (10)$$

$$S(t) = 0.0\,(unitless) \quad (11)$$

When transforming from NAD 83 to ITRF96, the HTDP program uses negative values obtained from these equations. The National Geodetic Survey and Geomatics Canada have jointly adopted these equations for relating ITRF96 and NAD 83 (M. Craymer, personal communication, 1998).[3] When transforming from ITRF96 to ITRF94, version 2.2 uses the values provided by the equation:

$$T_X(t) = T_Y(t) = T_Z(t) = R_X(t) = R_Y(t) = R_Z(t) = S(t) = 0.0 \quad (12)$$

that is, ITRF96 coordinates transform into identical ITRF94 coordinates, and *vice versa*. When transforming from ITRF94 to earlier ITRF realizations, version 2.2 uses equations based on the parameters published by Boucher and Altimimi (1996).

It follows from the previous discussion that HTDP can perform any coordinate transformation involving the official ITRF realizations and NAD 83. In addition, because HTDP incorporates crustal motion models, the software can transform positional coordinates of one epoch date in one reference frame to equivalent coordinates of another epoch date in another reference frame.

To present a particular application of this capability, consider a high-precision GPS survey involving some control points with known NAD 83 positions and an epoch date of 1 January 1997. Let it be assumed, however, that the satellite ephemerides to be used in processing the corresponding GPS data are expressed in ITRF96. Thus, to be rigorous, the positional coordinates of the control points should be transformed to ITRF96, such that the epoch date of the transformed coordinates equals the date of observation. Hence, the GPS processing software can perform all computations in ITRF96, and any new positions obtained from this processing will also be expressed in ITRF96 with their epoch date equal to the date of observation. Subsequently, HTDP can be applied to transform any such new positions from ITRF96 to another reference frame and to another epoch date, as desired.

# Concluding Remarks

The word "dynamic" may be attributed to the HTDP software for several reasons. The software merits this attribute primarily because it enables surveyors and others to deal rigorously with time-dependent positions on our dynamic planet. The attribute is also merited because the software has evolved rather dynamically over time. Since June 1992 when NGS released the initial version of HTDP, the agency has enhanced this software through a progression of 12 subsequent versions. Collectively, these subsequent versions have introduced numerous new and/or improved numerical models for crustal motion. They have also introduced additional capabilities, most notably, the capability to work with the various ITRF realizations as well as with the NAD 83 reference frame. As in the past, HTDP may be expected to continue evolving, so as to keep pace with the ever improving accuracy with which surveyors and others can position points.

The Fortran-77 source code for the current HTDP version is available, together with the documentation, via the Internet at <http://www.ngs.noaa.gov/PC_PROD/pc_prod.html>. Also from this Web site, surveyors and others can download the corresponding executable code in a form suitable for PC platforms. The documentation includes a set of instructional exercises designed to familiarize users with various applications of the HTDP software.

**ACKNOWLEDGMENTS**

In the spirit of scientific cooperation, individuals from many institutions readily shared their ideas, their data, and the results of their studies to support the development of the HTDP software. In particular, significant contributions have been provided by R. A. Bennett (Harvard-Smithsonian Center), M. W. Cline (NOAA), W. H. Dillinger (NOAA), J. D. D'Onofrio (NOAA), A. R. Drew (Minerals Management Service), L. Fenske (California Department of Transportation), S. J. Frakes (NOAA), J. G. Gergen (NOAA, retired), E. Grafarend (Stuttgart University), E. Herbrechtsmeier (NOAA), S. R. Holdahl (NOAA, retired), K. W. Hudnut (USGS), R. D. Hyndman (Geological Survey of Canada), D. D. Jackson (UCLA), M. Lisowski (USGS), C. Ma (NASA), D. C. McAdoo (NOAA), D. G. Milbert (NOAA), W. H. Prescott (USGS), C. M. Puskas (University of Utah), J. R. Ray (U.S. Naval Observatory), R. E. Reilinger (MIT), J. W. Ryan (NASA), J. M. Sauber (NASA), J.

[3] Note, in adopting zero for the value of S(*t*), representatives from the United States and Canada slightly modified the definition of NAD 83, by changing the scale of this reference frame from previous values used in these countries. Accordingly, the scale of NAD 83 now equals that of ITRF96.

C. Savage (USGS), C. R. Schwarz (NOAA), P. Segall (Stanford University), Z. K. Shen (UCLA), R. S. Stein (USGS), W. E. Strange (NOAA, retired), E. L. Timmerman (NOAA), C. A. Whitten (deceased), D. B. Zilkoski (NOAA), and E. G. Zurflueh (Nuclear Regulatory Commission).

## REFERENCES


Argus, D.F., and M.B. Heflin. 1995. Plate motion and crustal deformation estimated with geodetic data from the Global Positioning System. *Geophysical Research Letters* 22: 1973-6.

Bennett, R.A., R.E. Reilinger, W. Rodi, Y. Li, M.N. Toksoz, and K. Hudnut. 1995. Coseismic fault slip associated with the 1992 $M_W$ 6.1 Joshua Tree, California, earthquake: Implications for the Joshua Tree-Landers earthquake sequence. Journal of Geophysical Research 100: 6443-61.

Boucher, C., and Z. Altamimi. 1996. International Terrestrial Reference Frame. *GPS World* (September issue), pp. 71-4.

DeMets, C., R.G. Gordon, D.F. Argus, and S. Stein. 1990. Current plate motions. *Geophysical Journal International* 101: 425-78.

DeMets, C., R.G. Gordon, D.F. Argus, and S. Stein. 1994. Effect of recent revisions to the geomagnetic reversal time scale on estimates of current plate motions. *Geophysical Research Letters* 21: 2191-4.

Dixon, T., and A. Mao. 1996. How rigid is the stable interior of the North American plate? *Geophysical Research Letters* 23: 3035-8.

Ekstrom, E., R.S. Stein, J.P. Eaton, and D. Eberhart-Phillips. 1992. Seismicity and geometry of a 110-km-long blind thrust fault. 1. The 1985 Kettleman Hills, California, earthquake. *Journal of Geophysical Research* 97: 4843-64.

Federal Geodetic Control Subcommittee. 1994. *Input formats and specifications of the National Geodetic Survey data base: Volume I. Horizontal control data.* National Geodetic Survey, NOAA, Silver Spring, Md.

Fluck, P., R.D. Hyndman, and K. Wang. 1997. Three-dimensional dislocation model for great earthquakes of the Cascadia subduction zone. *Journal of Geophysical Research* 102: 20,539-50.

Holdahl, S.R., and J. Sauber. 1994. Coseismic slip in the 1964 Prince William Sound earthquake: A new geodetic inversion. *Pure and Applied Geophysics* 142: 55-82.

Hudnut, K.W. and 16 others. 1994. Co-seismic displacements of the 1992 Landers earthquake sequence. *Bulletin of the Seismological Society of America* 84: 625-645.

Hudnut, K.W. and 10 others. 1996. Co-seismic displacements of the 1994 Northridge, California, earthquake. *Bulletin of the Seismological Society of America* 86: S19-S36.

Jennings, C.W. 1975. *Fault map of California with locations of volcanoes, thermal springs and thermal wells.* California Division of Mines and Geology, San Francisco, Ca.

Larsen, S., R. Reilinger, H. Neugebauer, and W. Strange. 1992. Global Positioning System measurements of deformations associated with the 1987 Superstition Hills earthquake: Evidence for conjugate faulting. *Journal of Geophysical Research* 97: 4885-902.

Larson, K.M., J.T. Freymueller, and S. Philipsen. 1997. Global plate velocities from the Global Positioning System. *Journal of Geophysical Research* 102: 9961-81.

Lin, J., and R.S. Stein. 1989. Coseismic folding, earthquake recurrence, and the 1987 source mechanism at Whittier Narrows, Los Angeles Basin, California. *Journal of Geophysical Research* 94: 9614-32.

Lisowski, M., W.H. Prescott, J.C. Savage, M.J. Johnston. 1990. Geodetic estimate of coseismic slip during the Loma Prieta, California, earthquake. *Geophysical Research Letters* 17: 1437-41.

Ma, C., and J.W. Ryan. 1995. NASA space geodesy program—GSFC data analysis—1995: VLBI geodetic results 1979-1995.5. http://lupus.gsfc. nasa.gov/vlbi.html, Goddard Space Flight Center, Greenbelt, Md.

Okada, Y. 1985. Surface deformation due to shear and tensile faults in a half-space. *Bulletin of the Seismological Society of America* 75: 1135-54.

Oppenheimer, D., and 19 others. 1993. The Cape Mendocino, California, earthquake sequence of April, 1992: Subduction at the triple junction. *Science* 261: 433-8.

Savage, J.C., and W.K. Gross. 1995. Revised dislocation model of the 1986 Chalfant Valley earthquake, eastern California. *Bulletin of the Seismological Society of America* 85: 629-31.

Savage, J.C., M. Lisowski, M. Murray. 1993. Deformation from 1973 through 1991 in the epicentral area of the 1992 Landers, California, earthquake (MS = 7.5). *Journal of Geophysical Research* 98: 19,951-8.

Savage, J.C., M. Lisowski, and W.H. Prescott. 1991. Strain accumulation in western Washington. *Journal of Geophysical Research* 96: 14,493-507.

Segall, P., and Y. Du. 1993. How similar were the 1934 and 1966 Parkfield earthquakes? *Journal of Geophysical Research* 98: 4527-38.

Shen, Z.K., D. Dong, T. Herring, K. Hudnut, D. Jackson, R. King, S. McClusky, and L.Y. Sung. 1997. Crustal deformation measured in southern California. *EOS, Transactions of the American Geophysical Union* 78: 477-82.

Snay, R.A., and E. Herbrechtsmeier. 1994. The TDP-H91-CA model for historical horizontal deformation in California. *Manuscripta Geodaetica* 19: 180-98.

Snay, R.A., and T. Matsikari. 1991. Horizontal deformation in the Cascadia subduction zone as derived from serendipitous geodetic data. *Tectonophysics* 194: 59-67.

Snay, R.A., M.W. Cline, and E.L. Timmerman. 1987. Project REDEAM: Models for historical horizontal deformation. *NOAA Tech. Rep. NOS 125 NGS 42*, National Geodetic Survey, NOAA, Silver Spring, Md.

Snay, R.A., M.W. Cline, C.R. Philipp, D.D. Jackson, Y. Feng, Z.K. Shen, and M. Lisowski. 1996. Crustal velocity field near the big bend of California's San Andreas fault. *Journal of Geophysical Research* 101: 3173-85.

Stein, R.S., and G. Ekstrom. 1992. Seismicity and geometry of a 110-km-long blind thrust fault. 2. Synthesis of the 1982-1985 California earthquake sequence. *Journal of Geophysical Research* 97: 4865-84.

Stein, R.S., and M. Lisowski. 1983. The 1979. Homestead Valley earthquake sequence, California: Control of aftershocks and postseismic deformation. *Journal of Geophysical Research* 88: 6477-90. ■


## *Editor's Note

This article was published in the fourth issue of volume 58 of *Surveying and Land Information Systems*. It has been reprinted in this issue to provide corrected equations (4) and (10).